Journal of Applied and Natural Science
17(2), 802 - 809 (2025)
ISSN : 0974-9411 (Print), 2231-5209 (Online)
journals.ansfoundation.org

Research Article

Estimating extreme heat event over New Delhi Region, India using Satellite Data

Mohammad Suhail
Center of Applied Remote Sensing and GIS Applications, Samarkand State University, Samarkand, Uzbekistan
Mohd. Nazish Khan*
Department of Physical Geography and Natural Resources, Samarkand State University, Samarkand, Uzbekistan
Sachli Ganiyeva
Department of Geomatics, Azerbaijan University of Architecture and Construction, Baku, Azerbaijan
Abdumuminov Bakhodir Odinaevich
Department of Geography, Termez State University, Termez, Uzbekistan
Dilawez Ali
Department of Geology, Samarkand State University, Samarkand, Uzbekistan

*Corresponding author: nazishgeo@gmail.com

Article Info
https://doi.org/10.31018/jans.v17i2.6477
Received: December 26, 2024
Revised: May 30, 2025
Accepted: June 05, 2025

How to Cite
Suhail, M. *et al.* (2025). Estimating extreme heat event over New Delhi Region, India using Satellite Data. *Journal of Applied and Natural Science*, 17(2), 802 - 809. https://doi.org/10.31018/jans.v17i2.6477

Abstract
On May 26, 2024, Delhi experienced an extreme heat event, with temperatures soaring to record-breaking levels, exceeding 52°C, which was later revised to 46°C (114.8°F) by the India Meteorological Department.Amidst the controversy surrounding sensor failures, this study examines land surface temperature (LST) in Delhi using Landsat 9 OLI and MODIS Aqua data, focusing on the extreme heat event of May 26, 2024. This date was selected due to anticipated extreme heat and the availability of data. Satellite observations revealed temperatures as high as 56°C, with distinct spatial variations across Delhi. The western region recorded the highest temperatures, while the eastern region, influenced by the Yamuna River, exhibited cooler conditions. Emissivity values from Landsat (0.970–0.984) and MODIS (0.973–0.987) were analyzed, showing a strong correlation with surface temperatures: lower emissivity values corresponded to greener areas and lower temperatures, whereas higher values were linked to elevated temperatures. The study highlights the impact of surface characteristics on thermal behavior and underscores the role of urban heat islands (UHIs), particularly in northwestern Delhi. These UHIs, driven by industrial activity, dense settlements, and low-albedo materials, resulted in 2–4°C temperature differences between urban and rural areas, posing health risks to vulnerable populations. Mitigation strategies such as expanding green spaces and relocating high-emission industries are recommended to alleviate these risks. Despite the absence of field data, global studies validating Landsat and MODIS-derived LST support the accuracy of this study's findings. Thus, the spatial pattern of LST remains reliable even with minor errors ranging from 1 to 2 °C. The study will help for strategic planning and mitigation measures to address extreme heat events in urban areas.

Keywords: Extreme heat event, Land Surface Temperature, Landsat, Modis, Delhi

INTRODUCTION

The phenomenon of extreme heat conditions in megacities has captured significant attention from the scientific community, with a concentrated effort to dissect both the causative factors and the resultant impacts of such conditions. Despite this concerted focus, the incidence of sudden climate heat outbursts remains an area inadequately explored within current research paradigms. Scholars including Armson *et al*. (2012), Chen and Lu (2014), White *et al*. (2014), Abrams *et al*. (2015), Berger *et al*. (2017), and Nda *et al*. (2018) have underscored the critical need for more in-depth investigations into these abrupt and severe heat events. Their collective work emphasizes the necessity of unravelling the underlying mechanisms and broader implications of these intense thermal episodes to inform effective mitigation and adaptation strategies in urban environments. Extreme heat events are characterized by summertime temperatures that are significantly hotter and/or more humid than the average for that time of year in a given location. These conditions can have detrimental effects on the health of the natural world, particularly humans, leading to cases of heat exhaustion, heat stroke, cramping, and even death. Moreover, several studies describe the phenomenon of urban heat islands (UHI) as a leading cause of unprecedented severe heatwave conditions, which often prevail in parts of north India.This effect is due to the production and absorption of heat by urban surfaces, which disrupts airflow and alters the environment's aerodynamic, thermal, moisture, and radiative characteristics. These changes are driven by factors such as buildings, roads, and other infrastructure that absorb and retain heat (Gunawardena *et al*., 2017; Yang *et al*., 2019; Suhail *et al*., 2019; Nugroho *et al*., 2022).Previous research has demonstrated the effectiveness of remote sensing datasets for studying land surface temperature, urban heat islands, and other associated phenomena in both small and large cities, i.e., Singapore, Guangzhou, Delhi, Bengaluru (Weng *et al*. 2004; Mallick *et al*. 2013; Ailian *et al*. 2014; Grover and Singh 2015; Shahfahad *et al*. 2023).

However, amid the publication of controversial temperature data claiming that Delhi recorded its highest-ever temperature of 52.9 degrees Celsiuson May 26, 2024 (Anand, 2024; Dayal, 2024), subsequently revised with new temperature data indicating a reading of approximately 49.1 degrees Celsius. This data was later deemed an outlier, prompting an investigation to provide more accurate information. The India Meteorological Department (IMD) reported that several Indian cities recorded their highest maximum temperature on May 28. These include Agra (Uttar Pradesh), Bhatinda (Punjab), Churu (Rajasthan), Rewa (Madhya Pradesh), and among others (Anand, 2024). Experts attribute the city’s vulnerability to its location, large population, scattered vegetation, and significant construction over the last two decades. The built-up area has increased from 31.4% in 2003 to over 38% in 2022 (Dayal, 2024). Typically, the region experiences heat waves in May and June, with temperatures rarely extending into July and generally ranging between 45 and 49.1 degrees Celsius.Amid claims and counterclaims regarding the accuracy of the extreme temperature event in Delhi, the present study was initiated to determine the actual temperature and validate the assertions of government departments. The objectives included identifying the causes of this extreme event, understanding its spatial distribution, investigating why this unprecedented event occurred, and exploring strategies to address similar occurrences in the future.

MATERIALS AND METHODS

Study area

Delhi, the capital city of India, recorded an exceptionally high temperature on May 26, 2024, making it the focus of this study. The city is situated between 28° 14' 30.00" N, 76° 41' 0.00" E and 29° 0' 0.00" N, 77° 37' 15.00" E. Located on the banks of the Yamuna River, Delhi lies at an altitude ranging from 213 to 305 meters above mean sea level. The city spans an area of approximately 1483 square kilometers and has been experiencing an annual population growth rate of 4.63 percent (Fig.1).

Delhi ranks as India's most populous metropolitan city and holds the second position globally with a density of 1484 persons per square kilometer. This density underscores the significant levels of urbanization and industrialization in and around Delhi, which profoundly impact local weather patterns (Delhi Economic Survey, 2023). The city experiences three distinct seasons: winter (November to February), summer (March to June), and monsoon (July to October). While the monsoon season typically spans from June to September, Delhi received approximately 87% of its total rainfall during this period.

Data source and methodology

The present study used Landsat 9 OLI and MODIS Aqua (Moderate Resolution Imaging Spectroradiometer) data to extract Delhi's land surface temperature. MODIS features two sensors, i.e., Terra and Aq-

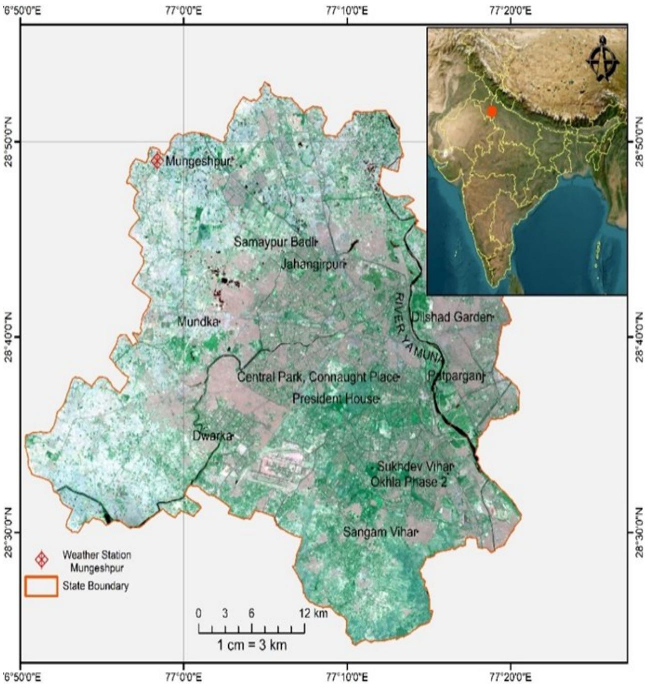

Fig. 1. *Location map of the study area*

ua. Terra orbits from north to south across the equator in the morning, while Aqua moves from south to north in the afternoon. Together, Terra MODIS and Aqua MODIS scan the entire Earth's surface every 1 to 2 days, capturing data in 36 spectral bands. Further, Landsat 9, which has been in orbit since September 2021 and operational since February 2022, is equipped with two sensors: the Thermal Infrared Sensor-2 (TIRS-2) and the Operational Land Imager 2 (OLI 2), featuring two thermal infrared bands. These datasets have shown promising results for global land surface temperature (LST) measurements, as evidenced by various studies (Barsi *et al*., 2014; Michael *et al*., 2015; Twumasi *et al*., 2021; Niclòs *et al*., 2023).Therefore, the remote sensing datasets were located and acquired from USGS Earth Explorer, specifically for May 26 2024, to carry out the analysis.The algorithm was developed in ArcGIS 10.5 using the Model Maker tool and is designed specifically for processing LANDSAT 9 and MODIS–Aqua data due to its complexity. Landsat 9 data is freely available on the USGS Earth Explorer website. This study used TIR band 10 to estimate brightness temperature (T_B) and bands 4 and 5 to calculate the normalized difference vegetation index (NDVI).

The entire process of calculation was completed, ad seriatim, in six steps viz., top of atmospheric spectral radiance (TOAR), radiance to at sensor temperature (T_B), normalized difference vegetation index (NDVI), fraction of vegetation cover (FVC), land surface emissivity, and land surface temperature. The land surface temperature was obtained from the equation as follows (Suhail, *et al*, 2019):

$$T_{LS} = \frac{T_B}{\left[1+\left\{\left(\frac{\lambda T_B}{\rho}\right)\ln(\varepsilon_\lambda)\right\}\right]} \qquad \text{eq.1}$$

Where T_{LS} is land surface temperature in Celsius (°C), T_B is at sensor temperature (°C), λ is the central wavelength of emitted radiance (λ = 10.895) (Sayler and Glynn, 2022), ε_λ is land surface emissivity, and ρ is the plank constant (calculated as 1.438 X 10^{-2}mK) (Avdan and Jovanovska, 2016). The T_B wasobtained from eq.2 as (USGS, Anonyms):

$$T_B = \frac{K_2}{\ln\left[\left(\frac{K_1}{TOAR}\right)+1\right]} - 273.15 \qquad \text{eq. 2}$$

Where K1 and K2 are conversion constants for band-specific conversion into temperature obtained from the metadata file of Landsat – 9. The land surface emissivity was obtained from eq.3 as (Sobrino, *et al*., 2004):

$$\varepsilon_\lambda = \varepsilon_{v\lambda}(F_{VC}) + \varepsilon_{v\lambda}(1 - F_{VC}) + C_\lambda \qquad \text{eq. 3}$$

Where $\varepsilon_{s\lambda}$ and $\varepsilon_{v\lambda}$ are the emissivity values of soil and vegetation, respectively, while C_λ is the surface roughness constant taken as 0.005 (Sobrino and Raissouni, 2000). Further, these conditions can be rewritten as:

$$\varepsilon_\lambda = \begin{cases} \varepsilon_{s\lambda} & NDVI < NDVI_s \\ \varepsilon_{v\lambda}(F_{VC}) + \varepsilon_{s\lambda}(1 - F_{VC}) + C_\lambda & NDVI_s \le NDVI \le NDVI_v \\ \varepsilon_{s\lambda} + C_\lambda & NDVI \ge NDVI_v \end{cases}$$

Where FVC and NDVI are fractional vegetation cover and normalized difference vegetation index, respectively, and can be obtained as (Sobrino *et al*., 2004):

$$F_{VC} = \left(\frac{NDVI - NDVI_s}{NDVI_v - NDVI_s}\right)^2 \qquad \text{eq.4}$$

When NDVI is less than 0, it represents the water pixels and the corresponding emissivity is to be assigned as 0.991, while the NDVI value greater than 0.5 represents vegetation cover and is to be assigned the emissivity as 0.937. The land and bare soil pixels of NDVI ranged between 0 and 0.2 and assigned emissivity as 0.996. Moreover, the mid-range between 0.2 and 0.5 is considered as mixed pixels of soil and vegetation. Accordingly, the entire image was called for the emissivity values. Further, the NDVI for Landsat OLI (operational land imager) – 9 was obtained from the equation (Berra *et al*., 2019):

$$NDVI = \left(\frac{NIR\,(B5) - Red\,(B4)}{NIR\,(B5) + Red\,(B4)}\right) \qquad \text{eq.5}$$

Where NIR and Red are the near-infrared and red bands of the OLI sensor respectively. Lastly, the top of the atmospheric spectral radiance can be obtained from the equation proposed by the United States Geological Survey (USGS) website (USGS, Anonyms) for Landsat – 9 as hereunder:

$$TOAR = M_L Q_{CAL} + A_L - C_B \qquad \text{eq.6}$$

Where M_L and A_L are band-specific multiplicative and additive rescaling factors, respectively, while Q_{CAL} is a standardized pixel value, and C_B is band calibration bias, as suggested by Avdan and Jovanovska (2016).

RESULTS AND DISCUSSION

Government statistics presented contradictory Fig.1s for the highest temperature observed on May 26, 2024. The India Meteorological Department (IMD) initially reported a temperature of 52.9 degrees Celsius for that Wednesday, but later revised Fig.1 to 49.9 degrees Celsius, attributing the discrepancy to a sensor failure at the Mungeshpur weather station (PIB, 2024; https://pib.gov.in/PressReleaseIframePage.aspx?PRID=2022142). This inconsistency raises significant concerns about the reliability and accuracy of the reported information. Media outlets have also questioned the revised data, suggesting it may not be accurate. This dubious information prompted the current study to verify the claims and provide accurate temperature estimates. The investigation included demonstrating techniques and satellite sensors used to retrieve temperature data. Analysis revealed that both Landsat and

Table 1. Showing the details of data acquisition, its characteristics, and metadata (https://www.usgs.gov/landsat-missions/landsat-9; https://lpdaac.usgs.gov/data/get-started-data/collection-overview/missions/modis-overview/)

Satellite	Sensor	Datasets	Date of Acquisition	Spatial Resolution	Rescaling Factor		Thermal Constant	
					M_L	A_L	K_1	K_2
Landsat – 9	TIRS	Band 10	26.05.2024	30 m	0.00038	0.1000	799.0284	1329.241
	OLI	Band 4	26.05.2024	30 m	0.009735	-48.6757	N/A	N/A
		Band5	26.05.2024	30 m	0.005967	-29.8334	N/A	N/A
MODIS	Auqa	LST Product	26.05.2024	1 km	0.002	N/A	Version 0.61 MYD11A1 v06 (LST and B31 & B32 emissivity product)	
		Band 31	26.05.2024	1 km	0.002	0.49		
		Band 32	26.05.2024	1 km	0.002	0.49		

MODIS recorded temperatures reaching approximately 56 degrees Celsius, slightly higher than the initial IMD estimates. This study highlights the importance of reliable data collection and underscores the potential of satellite technology in providing accurate environmental measurements.

The land surface temperature (LST) over Delhi was obtained using Aqua (MODIS) and TIRS-2 (Landsat-9) imagery. Fig.1s 2b and 2d showed that temperatures across most of the city exceeded the average normal temperature of 39.9 degrees Celsius forMay.Furthermore, distinct urban heat island (UHI) effects were prominently observed in the western and northern regions of the city, indicating localized areas of significantly higher temperatures.Global research indicates that urban heat islands (UHIs) can create temperature differentials of 2–4°C between urban centers and their rural surroundings (Suhail, 2016). These elevated temperatures pose substantial health risks to urban populations, especially to vulnerable social groups such as the elderly, children, and low-income communities. The increased heat can exacerbate heat exhaustion, heatstroke, and respiratory issues. However, implementing mitigation strategies, such as increasing green spaces, improving urban planning, and enhancing building materials, can significantly reduce these risks and improve urban residents' health outcomes. Analysis of Fig.1s 2a and 2c reveals that Landsat-derived emissivity values range between 0.970 and 0.984, while MODIS-derived emissivity values range between 0.973 and 0.987.

The analysis showed that Delhi was distinctly divided into two temperature zones, i.e., the eastern region, depicted in green, had comparatively lower temperatures, while the western region, shown in gamboge, experienced the highest temperatures. Particularly, the location of the Mungeshwar weather station coincided with the high-temperature region due to rapid industrialization and weakening of western disturbances (Fig.3). Similarly, MODIS data reflected a comparable temperature distribution across Delhi. The eastern periphery exhibited the lowest temperatures, while the highest was estimated at 56.43 degrees Celsius. The average temperature for the entire city ranged between 37.97 and 56.43 degrees Celsius on May 26, 2024. Central and eastern Delhi showed relatively lower temperatures, which is attributed to the presence of the Yamuna River, which transects the region, particularly at the eastern periphery. This river's cooling effect helps mitigate these areas' urban heat island phenomenon. Additionally, the southwestern region, particularly the Nazafgarh area, exhibited higher temperatures due to dense industrial and commercial activities. In contrast, Dwarka, situated just below Nazafgarh, experienced comparatively lower temperatures on May 26, 2024. This disparity is attributed to Dwarka's well-developed infrastructure and significant green spaces, contributing to temperature mitigation. Furthermore, in the northern region near the Mungeshpur weather station, certain parcels of land are undergoing constant alteration and economic activities, leading to higher recorded temperatures compared to other parts of Delhi. This continuous development and industrial activity in the vicinity of the Mungeshpur weather station exacerbate the urban heat island effect, resulting in elevated temperatures. Many earlier studies indicate a persistent trend of urban heat islands, particularly in northwestern Delhi. These areas are dominated by bare surfaces, asphalt, low-albedo materials, impervious rocks, high-density buildings, construction materials, and extensive road networks (Nancy *et al*., 2022). Additionally, the heat generated by industrial cooling systems contributes to elevated temperatures.

The capital has also experienced unprecedented severe heatwaves, predicted for North and Central India as the monsoon season approaches. These heatwaves often bring excessive heat before the downpours begin. Sudden heat outbreaks are possible when long and persistent heatwaves affect the region. To mitigate these sudden heat outbreaks, several measures can be undertaken. Reforesting the area can help reduce surface temperatures and improve the overall urban climate. Relocating high-emission industries to less populated areas or implementing stricter emission controls can also significantly lower local temperatures. These strategies should be part of a long-term strategic plan to create a more sustainable and resilient urban environment.

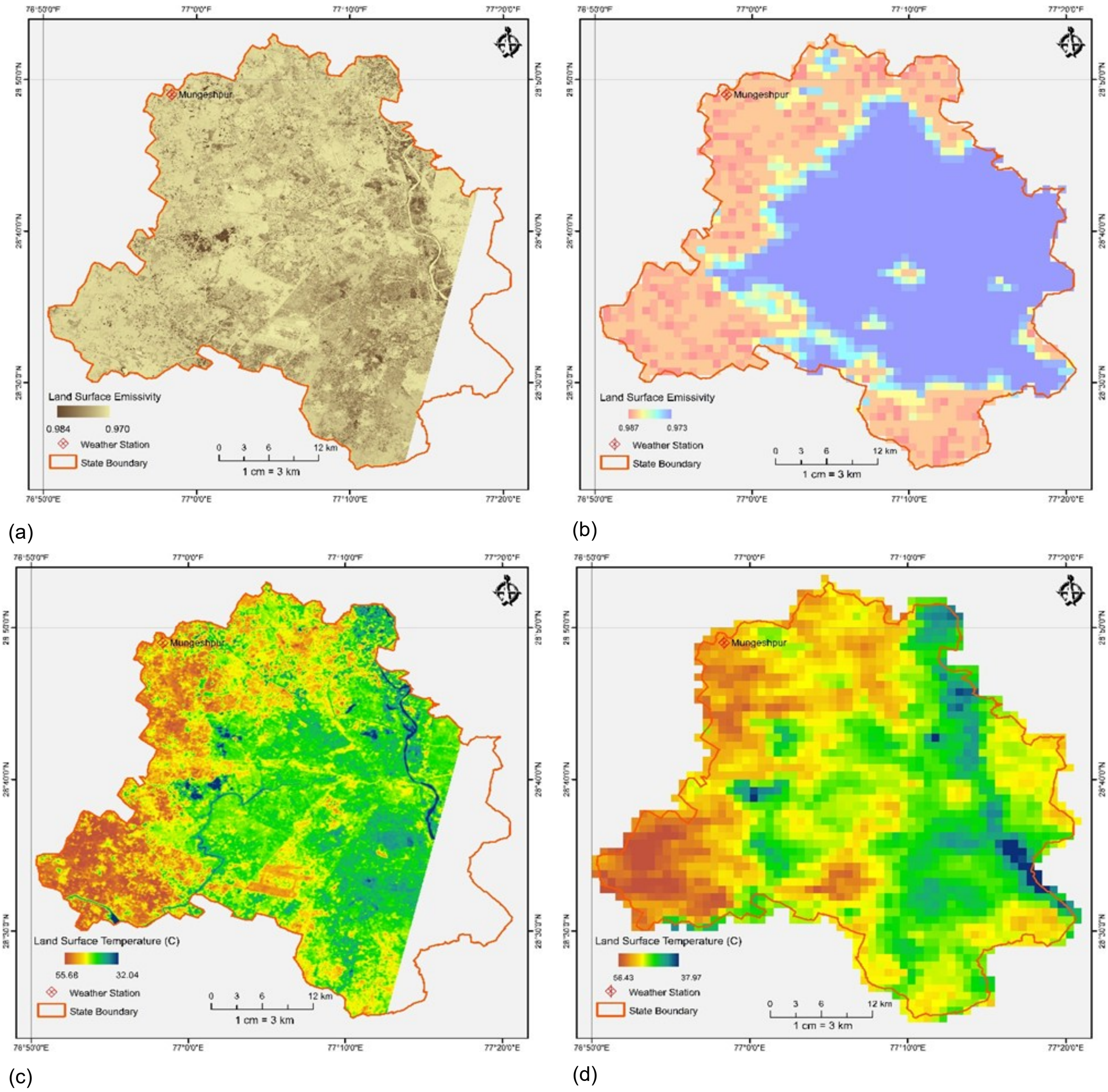

Fig. 2. *Spatial Distribution of Land Surface Emissivity and Temperature as obtained from Landsat (a & b), and MODIS (c & d), respectively*

Validation

Given the questionable nature of the claim and the reported sensor failure, validating the present assertion through field-based observation appears unlikely. Moreover, this weather event was unpredictable and extreme. However, in studies utilizing satellite-derived temperature retrieval, product validation is imperative. Errors in estimates often stem from instrumentation, emissivity, and cloud proximity. Assuming no instrument error due to continuous calibration by the Landsat research team, emissivity values were meticulously considered before LST estimation. However, the impact of cloud proximity was not factored in, as the data were devoid of clouds throughout the scene. Several international organizations and scientific teams, such as the Jet Propulsion Lab and NASA, have rigorously validated Land Surface Temperature (LST) results. These validated products encompass all Landsat satellite series and are globally recognized. A study analysed transmission and cloud proximity to assess Land Surface Temperature (LST) errors under different conditions. Results indicated that 30% of validation data have root-mean-squared errors (RMSEs) of less than 1 K, while 62% have RMSEs below 2 K. These minimal errors are unlikely to significantly impact the outcomes of the present result. A LST uncertainty model was also developed based on transmission and cloud proximity analysis, enabling users to select data points as need-

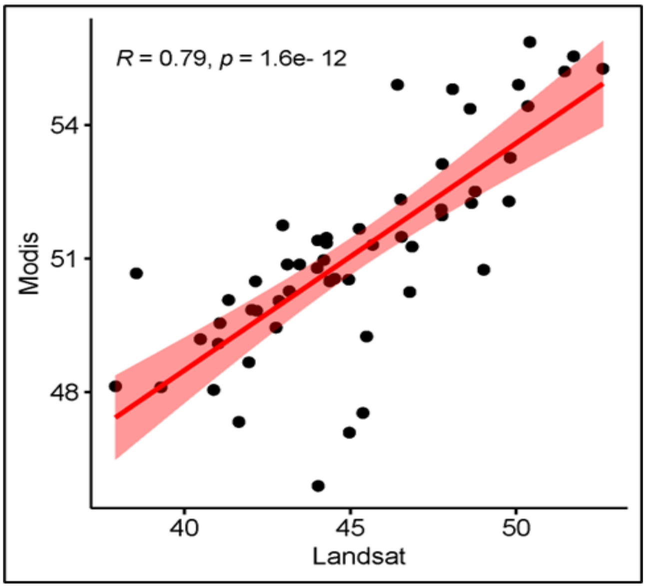

Fig. 3. *Correlation between estimated land surface temperature from TIRS–2 (Landsat 9) and Aqua (MODIS) on May 26, 2024*

ed. Several studies have validated the accuracy of Landsat and MODIS-derived Land Surface Temperature (LST) using various methods such as radiosondes, MODTRAN runs, and in situ emissivity measurements (Barsi *et al*., 2014; Laraby, 2017; Cook *et al*., 2014; Jimenez and Sobrino, 2004; Guillevic *et al*., 2017). These validations reported root-mean-square deviations (RMSD) of 2.2 K and 1.2 K for LST. Numerous global studies have also been conducted to validate Landsat-generated LST, with validation errors typically ranging from 1–2 K (Jiménez *et al*., 2009 & 2014; Tan *et al*., 2017; Duan *et al*., 2020). Despite these validations, the present study did not conduct LST validation due to the minimal effect of 1–2 K and the absence of field data and government records. Validation typically requires sophisticated instrumentation, precise ground estimates, and hourly real-time records, which were unavailable. The available daily average *in situ* records were deemed unsuitable for validation purposes. Furthermore, the spatial pattern of LST is unlikely to significantly change when considering the effects of errors ranging from 1 to 2 degrees Celsius in the present study.

Conclusion

Amid the claim that Delhi recorded its highest-ever temperature of 52.9 °C on May 26, 2024, which was subsequently revised as 49.1 °C, the study revealed significant insights about this extreme event. Remote sensing data from Landsat 9 OLI and MODIS Aqua was used to extract and analyze land surface temperature (LST). The results demonstrated the efficacy of these remote sensing datasets for LST measurement, contributing valuable insights into Delhi's temperature dynamics. The study found a strong correlation between emissivity and temperature, with lower emissivity linked to greener, cooler areas. The maximum temperature estimated was 55.68°C, with minimal error between TIRS–2 and Aqua data. However, it is slightly higher than initial IMD estimates. The study also identified significant urban heat island (UHI) hotspots, with temperatures across most of Delhi exceeding the average May temperature of 39.9°C. Emissivity values ranged between 0.970 and 0.984 for Landsat, and 0.973 and 0.987 for MODIS, supporting the accuracy of the temperature readings. The analysis revealed distinct temperature zones, with the eastern region showing lower temperatures (37.97-39.9°C) and the western region reaching up to 56.43°C. The Mungeshwar weather station recorded temperatures up to 56.43°C, particularly in industrial areas like Nazafgarh. Central and eastern Delhi had lower temperatures due to the Yamuna River. Weakened western disturbances and human-induced climate changes contributed to the rising temperatures. Reforestation, upgrading energy infrastructure, and relocating high-emission industries are recommended mitigation measures. However, Validating the extreme temperature claims for May 26, 2024, through field-based observations is challenging due to reported sensor failures.Despite minimal field data, global validations using various methods reported root mean square errors (RMSE) between 1.2 K and 2.2 K. Thus, the spatial pattern of LST remains reliable even with minor errors ranging from 1 to 2 degrees Celsius.

Conflict of interest

The authors declare that they have no conflict of interest.

REFERENCES

1. Abrams, J. F., & McGregor, G. R. (2015). Urban heat islands and climate change: A review of the literature. *Urban Climate*, 14, 1–18. https://doi.org/10.1016/j.uclim.2015.06.001
2. Ailian, C.X., Angela, Y., Ranhao, S., Liding, C. (2014). Effect of urban green patterns on surface urban cool islands and its seasonal variations, urban forestry & urban greening, 13(4), 646-654. https://doi.org/10.1016/j.ufug.2014.07.006.
3. Anand, N. (2024). India Sizzles at 50 degrees Celsius: A look at world record temperatures. Business Standard (Published June 2, 2024). Retrieved online from https://www.business-standard.com/india-news/india-sizzles-above-50-degree-celsius-a-look-at-world-temperatures-trends-124052900572_1.html
4. Armson, D., Stringer, P., Ennos, A.R. (2012). The Effect of tree shade and grass on surface and globe temperatures in an Urban area, Urban Forestry & urban greening, 11(3), 245-255. https://doi.org/10.1016/j.ufug.2012.05.002.
5. Avdan, U., & Jovanovska, G. (2016). Algorithm for auto-

mated mapping of land surface temperature using Landsat 8 satellite data. *Journal of Sensors,* 2016, 1-9. https://doi.org/10.1155/2016/1480307

6. Barsi, J.A., Schott, J.R., Hook, S.J., Raqueno, N.G., Markham, B.L., and Radocinski, R.G. (2014). Landsat-8 Thermal Infrared Sensor (TIRS) Vicarious Radiometric Calibration. *Remote Sensing*, 6, 11607–11626.
7. Berger, C., Rosentreter, J., Voltersen, M., Baumgart, C., Schmullius, C., Hese, S. (2017). Spatio-temporal analysis of the relationship between 2d/3d urban site characteristics and land surface temperature, remote sensing of environment, Volume 193, 225-243. https://doi.org/10.1016/j.rse.2017.02.020.
8. Berra, E.F., Gaulton, R., Barr, S. (2019). Assessing Spring Phenology of a Temperate Woodland: A Multiscale Comparison of Ground, Unmanned Aerial Vehicle and Landsat Satellite Observations. *Remote Sensing of Environment*, 223, 229–242.
9. Chen, Y., & Lu, R. (2014). Spatiotemporal changes in frequency and intensity of high-temperature events in China during 1961–2014. *Journal of Geographical Sciences*, 27(8), 1027–1043. https://doi.org/10.1007/s11442-017-1419-z
10. Cook, M., Schott, J.R., Mandel, J. and Raqueno, N. (2014). Development of an Operational Calibration Methodology for the Landsat Thermal Data Archive and Initial Testing of the Atmospheric Compensation Component of a Land Surface Temperature (LST) Product from the Archive. *Remote Sensing*, 6(11), 11244–11266.
11. Dayal, S. (2024). Why have temperatures reached record highs in India? Reuters (May 31, 2024). Retrieved online from https://www.reuters.com/world/india/why-have-temperatures-reached-record-highs-india-2024-05-31/
12. Duan, S.B., Li, Z.L., Zhao, W., Wu, P., Huang, C., Han, X.J., Shang, G. (2020). Validation of Landsat Land Surface Temperature Product in the Conterminous United States Using In Situ Measurements from SURFRAD, ARM, and NDBC Sites. *International Journal of Digital Earth,* 14(5), 640–660. https://doi.org/10.1080/17538947.2020.1862319
13. Government of Delhi. (2023). Economic Survey of Delhi 2023–24. https://static.investindia.gov.in/s3fs-public/2024-03/Economic%20Survey%20of%20Delhi%202023-24.pdf
14. Grover, A., Singh, R.B. (2015). Analysis of Urban Heat Island (UHI) in Relation to Normalized Difference Vegetation Index (NDVI): A Comparative Study of Delhi and Mumbai. *Environments,* 2, 125-138. https://doi.org/10.3390/environments2020125
15. Guillevic, P., Göttsche, F., Nickeson, J., Hulley, G., Ghent, D., Yu, Y., Trigo, I., Hook, S., Sobrino, J. A., Remedios, J., Román, M., & Camacho, F. (2017). Land surface temperature product validation best practice protocol (Version 1.0, p. 60). In P. Guillevic, F. Göttsche, J. Nickeson, & M. Román (Eds.), Best practice for satellite-derived land product validation. Land Product Validation Subgroup (WGCV/CEOS).
16. Gunawardena, K.R., Wells, M.J. & Kershaw, T. (2017). Utilizing Green and Blue Space to Mitigate Urban Heat Island Intensity, *Science of The Total Environment*, 584, 1040-1055. https://doi.org/10.1016/j.scitotenv.2017.01.158.
17. Jimenez-Munoz, J.C. and Sobrino, J. (2004). Error Sources on the Land Surface Temperature Retrieved from Thermal Infrared Single Channel Remote Sensing Data. *Int. J. Remote Sens.,* 27(5), 999–1014.
18. Jiménez-Muñoz, J.C., Cristóbal, J., Sobrino, J.A., Sòria, Ninyerola, G.M. and Pons., X. (2009). Revision of the Single-Channel Algorithm for Land Surface Temperature Retrieval from Landsat Thermal-Infrared Data. IEEE Trans. *Geosci. Remote Sens*., 47, 339–349.
19. Jimenez-Munoz, J.C., Sobrino, J. Skokovic, D., Mattar, C. & Cristobal, J. (2014). Land Surface Temperature Retrieval Methods from Landsat-8 Thermal Infrared Sensor Data. IEEE Geosci. *Remote Sens. Lett*., 11(10) 1840–1843.
20. Laraby, KG. (2017). Landsat Surface Temperature Product: Global Validation and Uncertainty Estimation. Thesis. Rochester Institute of Technology. https://www.cis.rit.edu/~cnspci/references/theses/phd/laraby2017.pdf.
21. Mallick, J., Rahman, A., & Singh, C. K. (2013). Modeling urban heat islands in heterogeneous land surface and its correlation with impervious surface area by using night-time ASTER satellite data in highly urbanizing city, Delhi-India. *Advances in Space Research*, 52(4), 639–649. https://doi.org/10.1016/j.asr.2013.04.025
22. Michael, A., Hiroji, T., Glynn, H., Koki, I., David, P., Tom, C., & Jeffrey, K. (2015). The Advanced Spaceborne Thermal Emission and Reflection Radiometer (ASTER) after fifteen years: Review of Global Products, *International Journal of Applied Earth Observation and Geoinformation,* 38, 292-301. https://doi.org/10.1016/j.jag.2015.01.013.
23. .
24. Nancy, Y., Nugroho, S. T., &Wonorahardjo, S. (2022). Effect of high-rise buildings on the surrounding thermal environment. *Building and Environment*, 207(Part A), 108393. https://doi.org/10.1016/j.buildenv.2021.108393
25. Nda, M., Adnan, M. S., Ahmad, K. A., Usman, N., Mohammad Razi, M. A., & Daud, Z. (2018). A review on the causes, effects and mitigation of climate changes on the environmental aspects. *International Journal of Integrated Engineering*, 10(4), 66–72.
26. Niclòs, R., Miguez-Macho, G., & Guijarro, J. A. (2023). The use of satellite remote sensing for monitoring urban heat islands: A global review. *Urban Climate*, 42, 100758. https://doi.org/10.1016/j.uclim.2022.100758
27. Sayler, K., & Glynn, T. (2022). Landsat 9 – Data user handbook (Version 1.0). U.S. Department of the Interior, United States Geological Survey.
28. Shahfahad, M., Talukdar, S., Rihan, M., & Rahman, A. (2022). Modeling urban heat island (UHI) and thermal field variation and their relationship with land use indices over Delhi and Mumbai metro cities. *Environmental Development and Sustainability.* https://doi.org/10.1007/s10668-022-02221-0
29. Sobrino, J. A., &Raissouni, N. (2000). Toward remote sensing methods for land cover dynamic monitoring: Application to Morocco. *International Journal of Remote Sensing*, 21(2), 353–366. https://doi.org/10.1080/014311600210876.
30. Sobrino, J. A., Jiménez-Muñoz, J. C., & Paolini, L. (2004). Land surface temperature retrieval from LANDSAT TM5. *Remote Sensing of Environment*, 90(4), 434–440. https://doi.org/10.1016/j.rse.2004.02.003.
31. Suhail, M., Khan, M. S., & Faridi, R. A. (2019). Assess-

ment of urban heat islands effect and land surface temperature of Noida, India by using Landsat satellite data. *MAPAN*, 34, 431–441. https://doi.org/10.1007/s12647-019-00309-9.

32. Tan, K., Liao, Z., & Du, P. (2017). Land surface temperature retrieval from Landsat 8 data and validation with geosensor network. *Frontiers in Earth Science*, 11(1), 1–12. https://doi.org/10.1007/s11707-017-0624-7.
33. Twumasi, Y. A., Fosu, M. A., & Osei, E. O. (2021). Estimation of land surface temperature from Landsat data in urban areas. *Remote Sensing*, 13(10), 1–18. https://doi.org/10.3390/rs13101999
34. U.S. Geological Survey (USGS) (2024). Using the USGS Landsat Level-1 data product. U.S. Geological Survey. Retrieved May 26, 2024, from https://www.usgs.gov/landsat-missions/using-usgs-landsat-level-1-data-product.
35. Weng, Q., Dengshang, L., & Jacquelyn, S. (2004). Estimation of land surface temperature and vegetation abundance relationship for urban heat island studies. *Remote Sensing of Environment*, 89(4), 467–483. https://doi.org/10.1016/j.rse.2003.11.005.
36. White-Newsome, J. L., McCormick, S., Sampson, N., Buxton, M. A., O'Neill, M. S., Gronlund, C. J., Catalano, L., Conlon, K. C., & Parker, E. A. (2014). Strategies to reduce the harmful effects of extreme heat events: A four-city study. *International Journal of Environmental Research and Public Health*, 11(2), 1960–1988. https://doi.org/10.3390/ijerph110201960
37. Yang, Y., Gatto, E., Gao, Z., Buccolieri, R., Morakinyo, T. E., & Lan, H. (2019). The "plant evaluation model" for the assessment of the impact of vegetation on outdoor microclimate in the urban environment. *Building and Environment*, 159, 106–151. https://doi.org/10.1016/j.buildenv.2019.05.029